CFD MODELLING AND EXPERIMENTAL VALIDATION OF AIR FLOW BETWEEN SPACES

D. Tang

Integrated Environmental Solutions Limited, Glasgow, UK

ABSTRACT

Studies of airflow between two adjacent spaces of building were carried out using CFD simulation. The results of CFD simulation were validated against test data set obtained from full-scale experimental tests. The agreement and discrepancy between the prediction and measurement results were discussed. Further numerical exercises were carried out to study under the conditions that were difficult to achieve by experiments and the results obtained were supplemented to the understanding of convective heat transfer between adjacent rooms.

KEY WORDS

CFD, Modelling, Full-scale experiments.

INTRODUCTION

Natural ventilation between spaces within buildings has always been an integral part of architectural design and is becoming even more important as it been seen as both means of energy efficiency and a way of improving occupant perceptions of the building. It has been seen that previous studies in this field are mainly experimental e.g. based on one-dimensional laminar flow analysis, similitude model experiments, as well as full size model tests. [Weber, 1983] [Brown, 1962] [Sandberg, 1989]

The technology of computational fluid dynamics (CFD) has been much evolving in the recent years and its application seen in numerous academic reports and industrial applications. Despite its popularity, the credibility of the simulation is still a prime issue to be addressed. Whilst experimental test is usually considered reliable, it suffers from high costs, instrumental limitations, human errors and very often it is not possible to conduct enough tests and to achieve required test conditions. To this end CFD simulation can be seen as an alternative and economical way to supplement, not to replace, experimental tests if the accuracy of the CFD modelling could be verified.

The purpose of this paper is to further explore this issue through extensive simulation and validation exercises.

THE EXPERIMENTAL FACILITY

In 1989 an international co-operative programme, the Annex 20.2, was carried for the study of inter-zone air flow and heat transfer. Within the programme a real-scale physical model was established for the measurement of airflow parameters in order to derive the formulations for the prediction of natural convective heat transfer between zones especially at low horizontal temperature. [Tang, et al. 1989]

The real-scale test facility was built within an existing indoor calorimetric chamber. The calorimetric chamber, sized *5.5mx2.5mx2.5m,* was made of *102m* polystyrene foam clad by 1mm aluminium sheets on either sides. A partition with an opening of *2.055mx1.25m* separated the test chamber into two zones. The end wall in the hot zone was heated by a uniform resistance film as heat source. The calorimetric chamber was isolated from the indoor environment by an extra enclosure with an air envelope in between. The air temperature within envelope space was

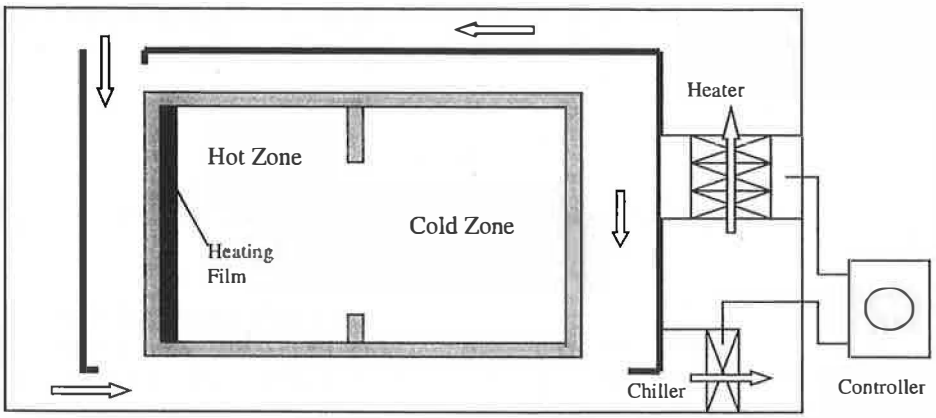

Figure 1. The experimental facility.

controlled by an air handling unit installed next to the test chamber and connected by supply and return conduits. Fig. 1 shows the concept of the experimental facility.

Totally 93 thermocouples were used to measure the surface and air temperatures, which included:

- Walls and partitions were divided into equal near square area and measured by a thermocouples located at the centre and from which area weighted surface temperatures were calculated for each surface.
- Air temperatures in each zone were measured simultaneously by thermocouples mounted on three vertical columns from which volume weighted average air temperatures were calculated. Only half of the space of the test chamber was measured based on the assumption of symmetry. Five thermocouples were used in each column. The heights for the thermocouples were: 0.25m, 0.75m, 1.25m, 1.75m and 2.25m, respectively.
- Air temperatures, velocity, turbulence intensity and pressure sensors were mounted on a remotely controlled servo device for measuring the corresponding variables on the plane of opening. Only half of the plane of the opening was measured based on the assumption of symmetry. Totally 17 locations were measured, with which 15 on the half plane and 2 were measured at top and bottom of the other half of the opening to ascertain the symmetrical assumption. The heights of the measurement locations were: 0.34m, 0.75m, 1.16m, 1.57m and 1.98m, respectively.

A data logger was used for data acquisition and as digital controller for controlling the air temperature within the envelope space. A PC was used to co-ordinate the operation of the data logger. Rigorous error estimation study prior to the tests indicated that the fluctuation of air temperature in the envelope space would cause significant system dynamic error. During all the steady-state tests, the fluctuation of air temperature within the envelope space was controlled at $\Delta T \leq \pm 0.5\,^{\circ}C$.

Steady-state measurement started after a 20-hour transition period by which the test chamber reached steady-state condition after each power setting. During the transition period, surface temperatures and air temperatures in the two zones were measured at a scanning interval of 15 minutes.

During the steady-state condition, all surface and air temperatures within the space were measured simultaneously for a three-hour period with a scanning interval of two minutes. At the end of the

measurement the arithmetic mean and standard deviation from the 90 values of each parameter were calculated.

Measurements of air temperature, velocity, turbulence intensity and pressure on the plane of the opening were carried out in a sequential manner based on the assumption of steady-state condition. It is assumed that these parameters would remain unchanged during steady-state condition and measurements made in different time can still be used as their time averaging values. At each position on the plane of opening, measurements for temperature, velocity, pressure and turbulence intensity were made for a period of 50 seconds with a scanning period of 0.5 second. It took approximately 40 minutes to complete the measurements of all the 17 positions.

After the measurement heat transfer study was carried out by deriving quantitatively the rate of convective heat transfer between the two zones. This was done by deducting from total heat loss of the cold zone calculated from the conductive heat loss through its boundary surfaces the radiative heat gain from the hot zone and the partition and the heat gain by conduction through the partition.

THE CFD SIMULATION MODEL

In the current study the Microflo CFD modelling system was used. Microflo is a general purpose CFD simulation system that is able to model time dependent air flow in three dimensional spaces internal and external of building, with buoyancy and turbulence effects, concentration dispersion, etc. In Microflo, the general air flow is characterised by a set of conservation partial differential equations of mass, momentum, energy and concentration, known as the Navier-Stokes equation. The transient version of Microflo was used in which the two-equation k-ε turbulence model was installed. Microflo provide facility for the definition of three kinds of thermal boundary conditions, i.e. constant temperature, heat flux and convective boundary; with or without forced air supply and extractions, this makes the CFD model to be identical to the test conditions to be modelled.

Details of the Microflo system can be found elsewhere. [Tang, 1998]

Figure 2 shows the geometric model used in the CFD simulation in which the surfaces of walls are numbered according the experimental arrangement.

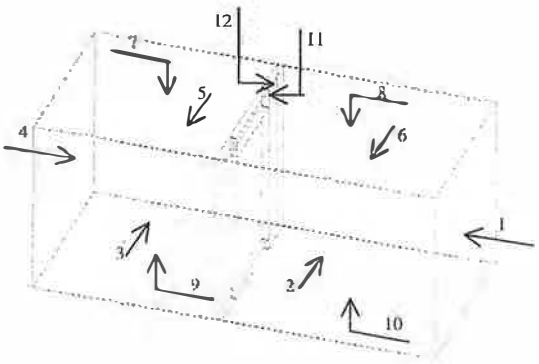

Figure 2. Geometry of the CFD model.

Other definitions of boundary conditions used in the CFD model include:

- Pure buoyancy driven flow, no forced air supply and extractor were defined;
- Power-law wall function was used for all the solid surfaces as velocity boundary condition.
- Convective boundary condition, i.e. boundary condition of the third-kind, was defined for all the surfaces except the heat source as temperature boundary condition;
- Pure convective heat source was used to model the electric heating film;
- Radiative heat exchanges within the space were accounted for by using the surface temperatures from the measurements.

Four CFD simulations were carried out with reference to the corresponding experimental tests in steady-state condition. The temperatures boundary conditions used in the simulations are given as follows:

Table 1. Results of experimental test 1.

Heating Power 147.52W					
Surface temperature:					
23.247	23.356	24.084	26.860	24.068	23.220
24.222	23.295	23.990	23.022	23.367	24.317

Table 2. Results of experimental test 2.

Heating Power 25.75W					
Surface temperature:					
25.772	25.695	27.166	31.378	27.904	25.769
27.381	25.893	26.870	25.460	26.053	27.453

Table 3. Results of experimental test 3

Heat Power 496.61W					
Surface temperature:					
32.047	31.975	34.374	41.847	34.298	31.999
34.839	32.277	33.819	31.368	31.510	34.925

Table 4. Results of experimental test 4

Heat Power 909.23W					
Surface temperature:					
42.082	41.995	45.762	57.400	45.686	41.953
46.570	42.492	44.946	40.996	42.920	46.804

Fig. 3 to 6 show parts of the results obtained from CFD simulation based on experimental test data set 1.

Fig. 3 shows the velocity profile taken from the central line cutting through the two zones.

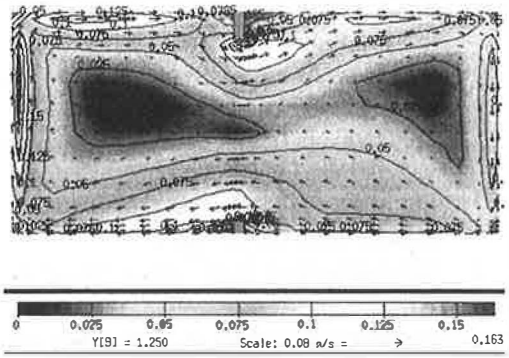

Figure 3. Central line velocity profile.

Fig. 4 shows the velocity profile taken near the top level of the doorway. It can be seen from Fig. 4 that the distribution of air velocity differs from the one-dimensional airflow pattern. This was caused by the change of directions of air stream caused by the restriction of the doorway.

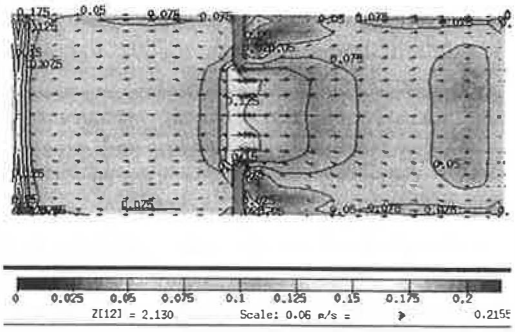

Figure 4. Velocity profile at top of the opening.

Fig. 5 shows the air temperature profile taken from the central line cutting through the two zones.

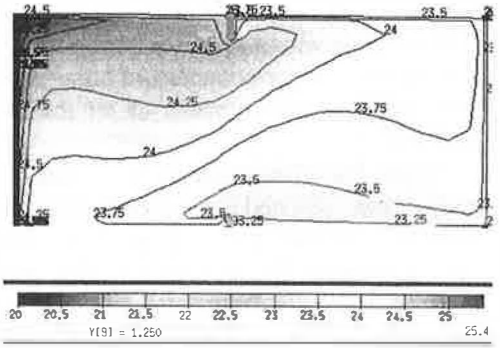

Figure 5. Central line temperature profile.

Fig. 6 and 7 show the numerical visualisation of air movement using the technique of particle tracking and animation by which the air streamlines were animated as 3D moving line objects. In fig 6 and 7 the movement of the streamlines show the air velocity and direction; the colour variations on each streamline show the change of air temperatures along the air flow paths. Fig. 6 shows the airflow streamlines viewed from the hot zone. Fig. 7 shows the airflow streamlines viewed from the cold zone in a close-up view.

The air flow patterns obtained from CFD simulations were in good agreement with the experimental observations. Both fig. 6 and 7 show that the air flow between the two zones in general formed a boundary layer of higher velocity flow along the

perimeter of the test chamber. They also show that the airflow pattern differs from the one-dimensional flow assumption in that there were large eddies occurred in both zones caused by the restriction of the doorway. Such large eddies then re-entered the opposite zone.

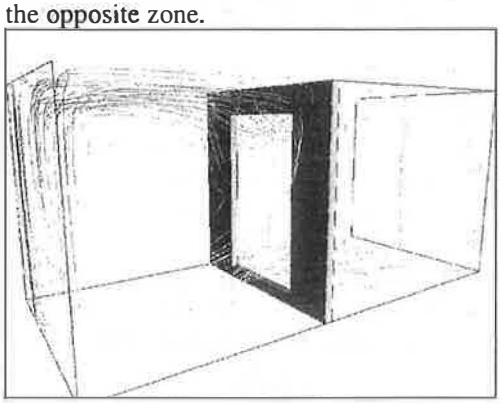

Figure 6. Air flow streamlines viewed from the hot zone.

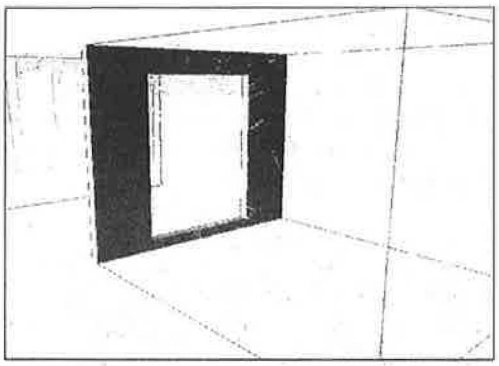

Figure 7. Air flow streamlines viewed from the cold zone.

VALIDATION AND DISCUSSION

Fig. 8 shows the experimental arrangement of the vertical columns where air temperatures were measured simultaneously. Measurements were also made on the plane of the opening in a sequential manner. Only half of the space and the plane of the doorway were measured based on the assumption of symmetry.

Extensive validation studies between the CFD simulation results and the experimental test data sets had been carried out for all the measuring locations and parameters. [IES, 1997] Part of the findings are summarised as follows:

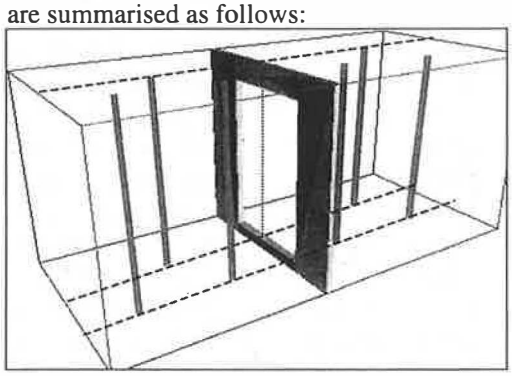

Figure 8 Locations of 3D air temperature measurement in the test chamber.

Temperature field

In general, temperature fields predicted by the CFD simulations are in good agreement with the measurements for most of the test locations and test conditions. Figure 9 to 20 show parts of the comparison results for selective locations in the test chamber.

Fig. 9 to 12 show the comparisons of air temperatures for the five vertical locations at the centre of the opening.

Fig. 13 to 16 show the comparisons of air temperatures for the five vertical locations at the centre of the hot zone. Fig. 17 to 20 show the comparisons of air temperatures for the five vertical locations at the centre of the cold zone.

As demonstrated in the aforementioned experimental study, the convective heat transfer between adjacent zones connected by opening of partition depends mainly on the temperature difference between the zones, the accuracy of CFD prediction using Microflo provides a useful mean for the heat transfer studies.

Velocity field

Fig. 21 to 24 show the comparisons of predicted and measured distribution of air resultant velocity on the five vertical locations at the centre of the opening. It can be seen that the discrepancy between

measured and predicted air velocity are significant near top and bottom of the doorway by which the measurements tended to be lower. This was also observed during the tests and considered that the cause may be due to the shape of the omnidirectional velocity sensor installed on the servo moving device which acted as an obstruction to the main air stream and thus caused local disturbance of airflow. This happened especially at the top and bottom of the doorway where flows were further restricted by the edges of the opening. Since the air temperature appears stratified vertically, the disturbance of airflow may not have direct effect on the air temperature field at the same level. However such explanations may need to be verified through further experiments.

Horizontal temperature difference

Difficulties were experienced during the experiments in trying to increase the horizontal air temperature difference between the two zones. Further CFD simulation studies discovered that the chances to increase horizontal temperature difference were low even if significant amount of heating and cooling sources were applied to the hot and cold zone, respectively. The reason for this was mainly due to the large size of the opening through which the warm and cool air were constantly exchanged and therefore compensated the temperature rises and falls in the corresponding zones. This in turn gave clear indication to the design of the experiment where expensive equipment and test failures may possibly be avoid.

CONCLUSION

Studies of airflow between two adjacent spaces of building using full-scale experiments and CFD simulations were introduced. The results of CFD simulation were validated against test data obtained from the full-scale experimental tests. Comparisons of the results between the CFD simulations and the experimental measurements were made and agreement and discrepancy between the two methods were discussed. Further CFD simulation exercises were carried out to investigate the conditions that were difficult to achieve by experiment for the studies of convective heat transfer between adjacent rooms.

REFERENCES

Brown, W.G. and Solvason, K.R. (1962) Natural Convection Through Rectangular Opening in Partition-1, Int. J. Heat Mass Transfer, vol. 5, pp.859-868.

IES, (1997) *Microflo Validation Report, IES Technical Series,* Integrated Environmental Solutions Ltd. Sept.

Sandberg, M. (1989) Flow Through Large Opening, IEA Annex 20.2 Task Communication.

Tang, D. (1998) Virtual Environment for the Prediction of Air Movement in Buildings. 6th International Conference on Air Distribution in Rooms, KTH, Stockholm, Sweden.

Tang, D. and Robberechts, B. (1989) Inter-zone Convective Heat Transfer and Air Flow Patterns, Report of Laboratory of Thermodynamics, University of Liege, March.

Weber, D. D. (1983) Similitude Modelling of Natural Convection Heat Transfer Through an Aperture in Passive Solar Heated Buildings, Ph.D. thesis, University of California, LA-8385-T.

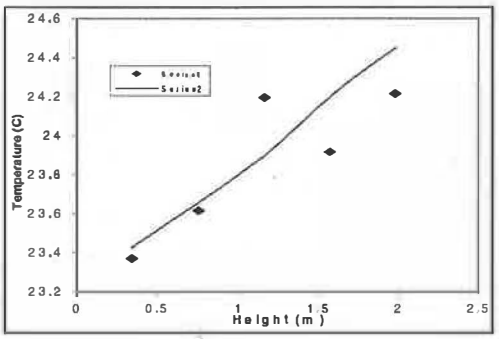

Figure 9 Test 1, temperature field at centre of opening.

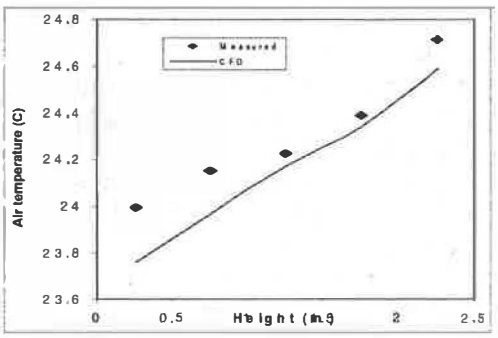

Figure 13 Test1, temperature field at centre of hot zone

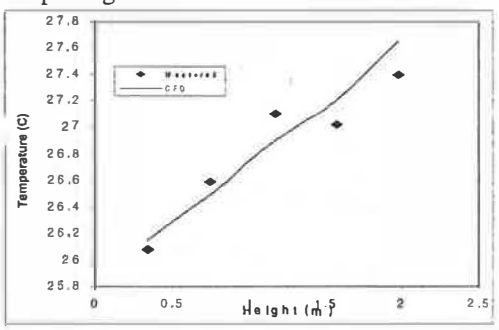

Figure 10 Test 2, temperature field at centre of opening.

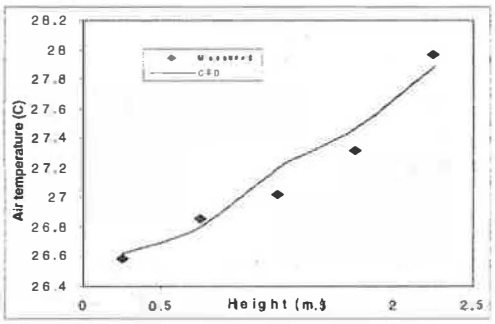

Figure 14 Test 2, temperature field at centre of hot zone

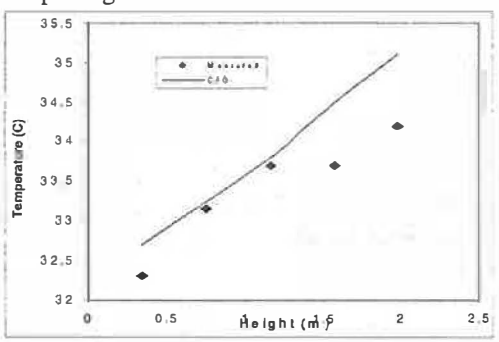

Figure 11 Test 3, temperature field at centre of opening.

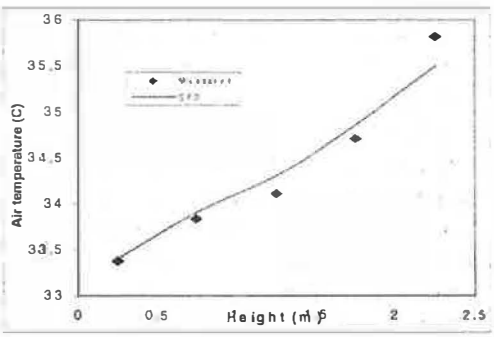

Figure 15 Test 3, temperature field at centre of hot zone.

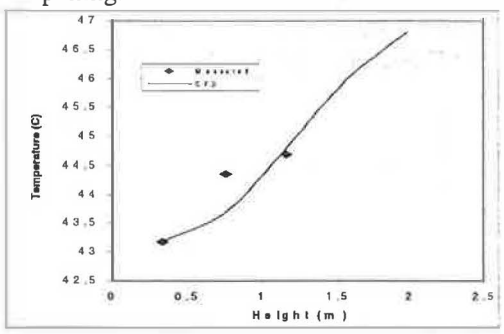

Figure 12 Test 4, temperature field at centre of opening.

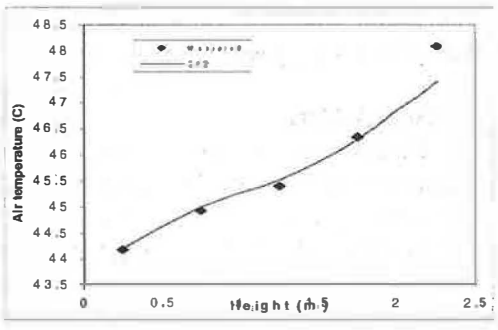

Figure 16 Test 4, temperature field at centre of hot zone.

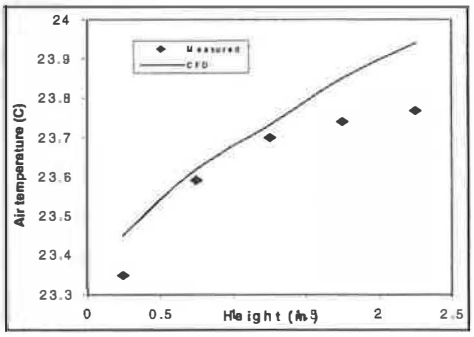

Figure 17 Test 1, temperature field at centre of cold zone.

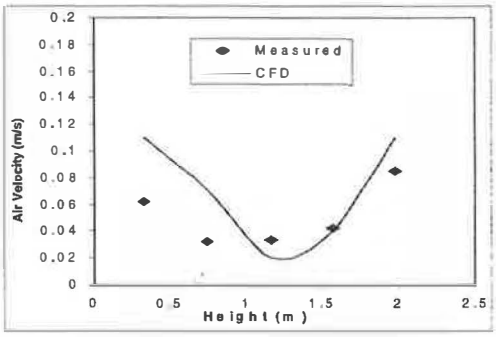

Figure 21 Test 1, velocity field at centre of opening.

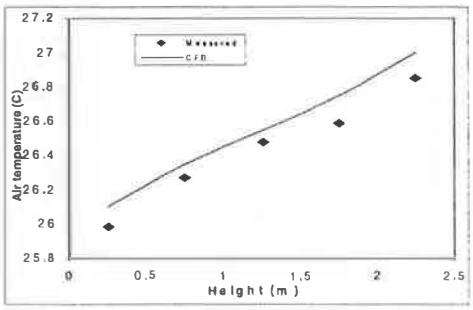

Figure 18 Test 2, temperature field at centre of cold zone.

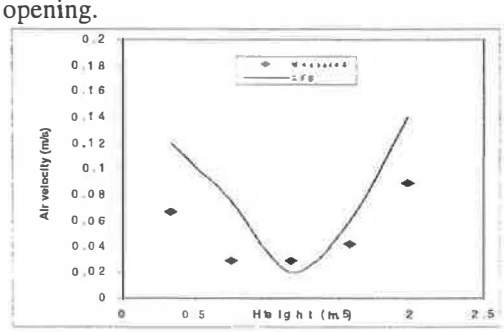

Figure 22 Test 2, velocity field at centre of opening.

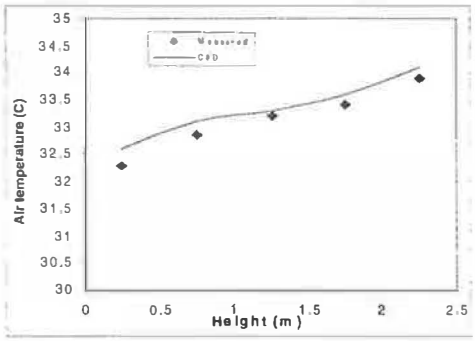

Figure 19 Test 3, temperature field at centre of cold zone.

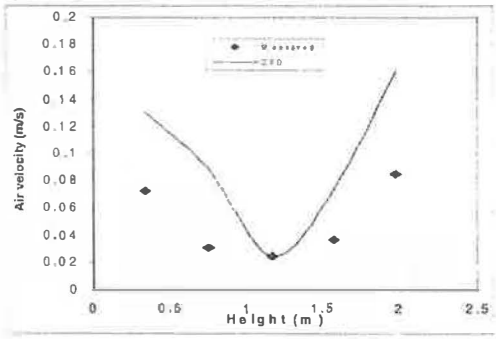

Figure 23 Test 3, velocity field at centre of opening.

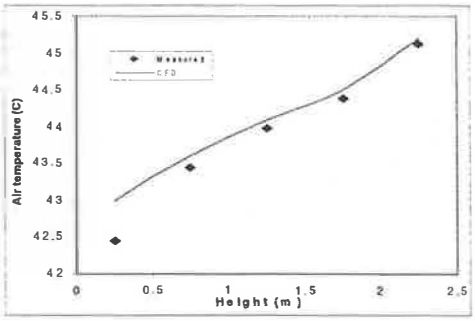

Figure 20 Test 4, temperature field at centre of cold zone.

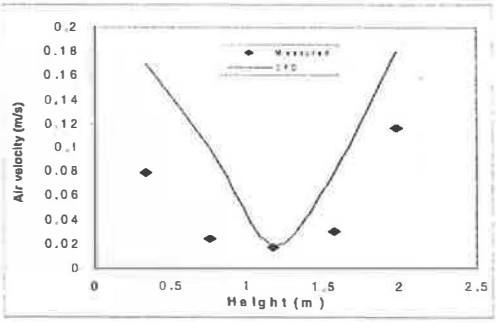

Figure 24 Test 4, velocity field at centre of opening.